SPLITTING FRAMES BASED ON HYPOTHESIS TESTING FOR PATIENT MOTION COMPENSATION IN SPECT

by

LINNA MA

A Thesis

Submitted to the Faculty

of the

WORCESTER POLYTECHNIC INSTITUTE

in partial fulfillment of the requirements for the

Degree of Master of Science

in

Computer Science

May 2006

Approved:

_____

Prof. Michael A. Gennert, Thesis Advisor

_____

Prof. Matthew O. Ward, Thesis Reader

_____

Prof. Michael A. Gennert, Head of Department

ACKNOWLEDGMENTS

My deepest gratitude to my supervisor, Prof. Michael Gennert. This thesis is to a large extent a results of his skillful guidance and encouraging support of my work. My sincere thanks to Prof. Matt Ward for agreeing to be the second reader of this thesis. I also thank UMass Medical School Nuclear Medicine group, for providing a work environment and their helpful comments. This project was funded by National Institute of Biomedical Imaging and Bioengineering R01 EB001457. Finally, heartfelt thanks go to my family for their immense support along the way.

ABSTRACT

Patient motion is a significant cause of artifacts in SPECT imaging. It is important to be able to detect when a patient undergoing SPECT imaging is stationary, and when significant motion has occurred, in order to selectively apply motion compensation. In our system, optical cameras observe reflective markers on the patient. Subsequent image processing determines the marker positions relative to the SPECT system, calculating patient motion. We use this information to decide how to aggregate detected gamma rays (events) into projection images (frames) for tomographic reconstruction.

For the most part, patients are stationary, and all events acquired at a single detector angle are treated as a single frame. When a patient moves, it becomes necessary to split a frame into subframes during each of which the patient is stationary. This thesis presents a method for splitting frames based on hypothesis testing. Two competing hypotheses and probability model are designed. Whether to split frames is based on a Bayesian recursive estimation of the likelihood function. The estimation procedure lends itself to an efficient iterative implementation. We show that the frame splitting algorithm performance is good for a sample SNR. Different motion simulation cases are presented to verify the algorithm performance. This work is expected to improve the accuracy of motion compensation in clinical diagnoses.

TABLE OF CONTENTS

LIST OF FIGURES

Figure **Page**

CHAPTER 1

INTRODUCTION

1.1 Problem Statement

Many patients undergo cardiac single photon emission computed tomography (SPECT) imaging every year. SPECT system is shown in Figure 1.1, 1.2 and 1.3. SPECT data acquisition requires the patient to remain still for a long time (around 15-20 minutes) to guarantee image quality. However, in clinical practice patients often move, introducing imaging artifacts. In the academic centers we know the body motion may occur in 25% of studies and that 5% of the time, patient motion is significant enough to cause artifacts which can mislead diagnosis [3, 4]. One study in T1-201 polar maps has shown that motion of single pixel ($6.4mm$) can induce significant artifacts [17].

Compensation strategies for motion in SPECT imaging, although commercially available, are inadequate for robust clinical usage. For example, currently there are some corrections for the attenuation and scatter physics effects. Also small, period patient motion such as respiration can lead to blurring and loss of resolution. But these corrections all need the patient motion compensation to remove the major patient shift factor for clinical usage. Larger motions such as patient shift lead to more serious artifacts that may mask or mimic perfusion defects. The use of external tracking devices for motion compensation, bringing information independent of SPECT data, is expected to be much more robust. In motion compensation, it is necessary to split frames accurately in order to get better motion compensation results.

We know SPECT data may be acquired in either of two modes: frame mode or list mode. In frame mode, a projection frame is produced at every detector angle. Individual photons, i.e. detected events, are not recorded separately, only in aggregate. The detector is stepped several degrees between frames until full 360^{deg} coverage is obtained. In list mode, each detected gamma ray (event), including timestamp is recorded in a file; hence

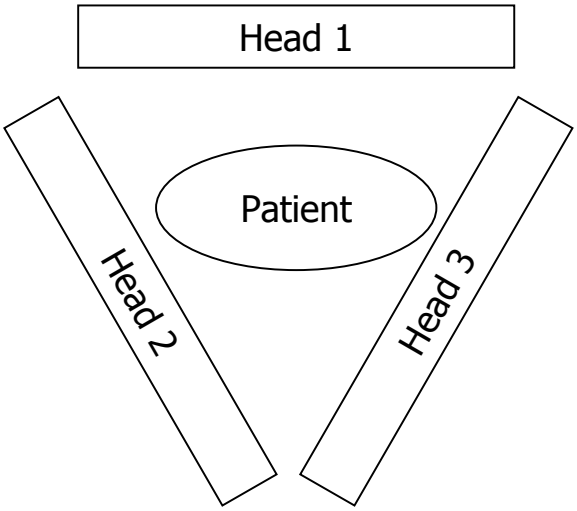

Figure 1.1. SPECT (Single Photon Emission Computed Tomography) Imaging

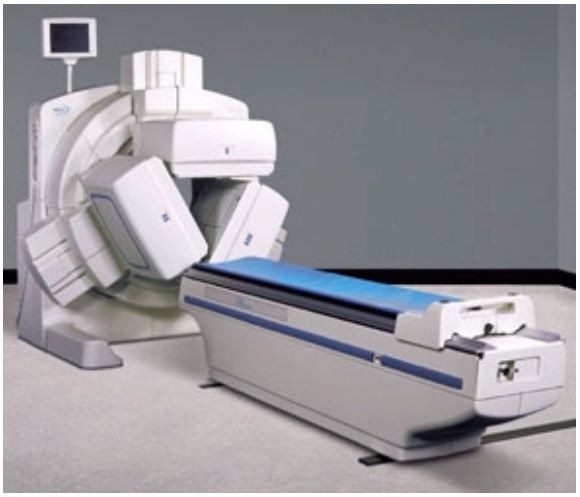

Figure 1.2. Phillips IRIX Gamma Camera

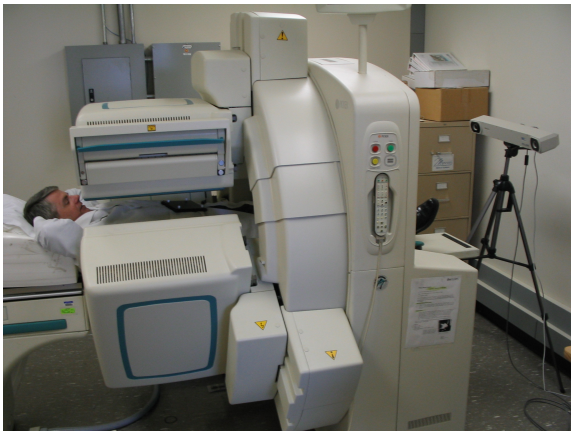

Figure 1.3. Polaris IR System View

the SPECT data comprises a large list. The list of events is adjusted to produce a corrected set of motion-free observations instead of the integrate projection image frame. List mode data may be converted to frame mode by summing all events at a given detector angle, producing a frame at that angle. So after the compensation work, we may do the list mode based reconstruction or do the frame mode based reconstruction after reformatting work.

When frame mode was used for motion compensation [2], patient motion at each frame is related to the initial patient position. This works well in if the patient only moves between frames, an impractical restriction. If SPECT data were acquired in list mode, and a new frame created whenever the patient moved, this splitting frame approach could succeed with any patient motion. Thus, the current problem is to split frames whenever significant patient motion is detected.

For the most part during list mode data acquisition, patients are stationary, and all events acquired at a single detector angle are treated as a single frame. When a patient moves, it becomes necessary to split a frame into subframes during each of which the patient is stationary. The detailed strategy for splitting frames accurately will be presented in the subsequent parts.

1.2 Thesis Outline

The thesis begins with an introductory chapter, where the splitting frames problem and the practical applications are discussed in general terms. The basic concepts and approaches introduced in this chapter are explained in the subsequent parts of the thesis.

The remaining five chapters of the thesis are organized in four parts, as described here: Chapter 2 reviews the previous work and background in motion compensation, our visual tracking system and the splitting frames combination solution; Chapter 3 focuses on the theory deduction and basic understand of splitting frames problem; Chapter 4 describes the algorithm implementation, pseudo code, and algorithm optimization work; Chapter 5 covers different patient motion situation, the case study experiments results and analysis; Chapter 6 discusses the future work and the thesis is concluded. All publications referred to in the thesis are compiled in the bibliography.

CHAPTER 2

BACKGROUND

The splitting frames strategy is expected to improve the accuracy of motion compensation in clinical diagnoses. We know in the academic centers, researchers usually make the "patients" comfortable and control the imaging environment. These "low-likelihood" patients are less likely to move than those who are more likely to have disease. In the clinical cases, actual patient motion would be one of the most important factors. Significant motion can result in the image artifacts that may be erroneously interpreted as perfusion defects. The false-positive interpretations with motion may be as high as 27 percent [13]. Although there are some real cardiac motions, but the significant cardiac motion is seldom. The image artifacts are mainly caused by the patient motion.

2.1 Motion Compensation

When patient undergoing SPECT, it is necessary to record the sequence of patient position in order to selectively apply motion compensation. A number of approaches have been developed to detect and correct for body motion using only emission data. Motion artifacts can be reduced by manual shifting of individual projection images before reconstruction. For example, Fitzgerald [7] suggested having the technologist or physician view the cine, sonogram, or linogram of the acquisitions and interactively move the projection data to compensate for motion. But the effectiveness of procedure is dependent on the operator and it is time-consuming. There are also many automatic or semiautomatic methods for motion compensation in SPECT studies. One way is to place external radioactive markers on the patient's body within the camera heads, and detect the motion of these markers. William J. Geckle [20] described an algorithm to track the center of the heart in successive projections and correct its motion based on realignment of the center to a fixed point in space. Barakat [16] proposed an algorithm to detect motion in projection data from triple

scan SPECT imaging. This algorithm permits the acquisition of three full sets of SPECT data which can be adequately combined in order to reconstitute a motion-free set of projection data. Fulton [18] uses full 3D reconstruction, which places some limitations on the nature or timing of the motion which can be corrected. In the motion correction with full 3D reconstruction, sometimes researchers have to assume the patient remains stationary during the acquisition of individual projection and only moves between projections. The above methods use frame data. That is, when the six cameras are at a fixed angle and a "frame" or image is acquired. Individual photons, i.e. detected events, are not recorded separately, only in aggregate. We tried list mode data based motion compensation [8]. The list of events is adjusted to produce a corrected set of motion-free observations instead of the integrate projection image frame. After the compensation and reformatting, we do 3D reconstruction based on the ordered subsets expectation maximization (OSEM) algorithm for comparison. In [18] Hutton proposed a method to model patient motion in reconstruction by dividing projection data into subsets where no motion occurs. In [15] Bruyant proposed a compensation method based on the knowledge of the patient state during list-mode SPECT data acquisition. Our splitting frames strategy, verifying motion decision, can be applied in either motion compensation approach in future.

In the whole system, by synchronizing with visual tracking system, SPECT diagnostic imaging is expected be improved. Usually the SPECT system scans 20-30 minutes, visual tracking system runs at the same time with 25frames/second acquisition speed. Since the optical cameras are synchronized with SPECT, the spheres(markers) as shown in Figure 2.1 on patient, can be observed to get the patient motion raw data. The raw motion will be imported to the splitting frames strategy, for applying motion compensation selectively.

2.2 Previous Work

Most previous approaches of making decision for patient motion have relied on acquired projection data and they detect motion with consistency checks or motion tracking. Our approach is based on optical tracking of the patient using a pair of web cameras to acquire stereo images. The stereo images are analyzed by a Visual Tracking System that records locations of stereo images on the patient surface over time. Patient surface motion can infer

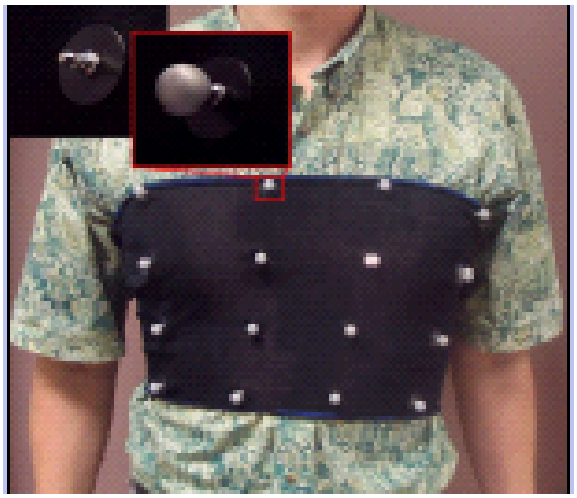

Figure 2.1. Reflective Markers on Black Garment - Objective

motion within the patient body, which will be used to correct for actual patient motion[12]. The cameras are directed at reflective markers placed on the surface of a tight fitting garment worn by the patient[14]. By comparing the positions of the spheres on patient body between time slots, we can record patient movement and get the patient position in 3D space. The splitting frames work is base on the whole system to verify and make decision for patient motion.

2.3 Splitting Frame Solutions Overview

This thesis presents a method for splitting frames based on hypothesis testing. Two competing hypotheses and probability model were designed. We propose to automatically decide if and where to split each frame, and consider recursive splitting of resulting sub frames. This splitting frames strategy for motion compensation can work well for any patient motion.

Whether to split frames is based on a Bayesian recursive estimation of the likelihood function. The estimation procedure lends itself to an efficient iterative implementation. We show that the frame splitting algorithm performance is good for a sample SNR. Different motion simulation cases are presented to verify the algorithm performance. After splitting frames for motion compensation, the selective motion may be applied to correct the SPECT

reconstruction. This work is expected to improve the accuracy of motion compensation in clinical diagnoses.

CHAPTER 3

STATISTICAL MODEL FOR SPLITTING TIME-SERIES FRAMES

In the problem of verifying patient motion, the motion decision is indirectly observable from the observed patient motion data in SPECT system, since the noise is in the observation of a real world phenomenon. Statistical estimation can deal with this problem. By introducing the recursive estimation, the motion decision is updated continuously after getting new sub-frames. With the Bayesian view on motion decision, both the sought parameters and observed motion are stochastic entities. In our Statistical model presented in the following sections, the patient motion decision and splitting frames decision can be inferred.

3.1 Model Construction based on Bayesian Theory

After synchronizing the visual tracking system with SPECT system, we have patient position data. For the patient position, we defined the hierarchical objective structure, shown in Figure 3.1. There are four objective levels. The first level is frame objective level , which indicates the aggregated frames we recorded for patient motion and need to be splitted. The second level is time objective level. Each frame corresponds to it's own recorded timestamp. The third level is image/sphere objective level. There are usually have N($N \approx 20$) spheres on patient body, which is monitored in SPECT system. The fourth level is patient motion objective level. The location(x, y, z) of each sphere indicates the motion in consequent time slots.

Two competing hypotheses can be acting for one frame, respectively:

H_0: There is no patient motion in this frame. Then the location of spheres on patient is the detected coordinates with noise which is assumed to be a zero-mean Gaussian noise with variance σ^2.

H_1: There is patient motion in this frame.

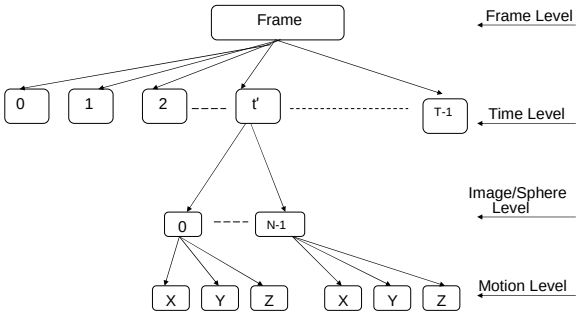

Figure 3.1. Hierarchical Data Structure for Splitting Frames

3.2 Maximum Likelihood Estimation

We need to decide whether there is patient motion based on two probabilities $Pr(H_0|\mathbf{X})$ and $Pr(H_1|\mathbf{X})$, where $\mathbf{X}$ is the observed data. From Bayesian theory, we can obtain the following equations.

$$Pr(H_1|\mathbf{X}) = \frac{Pr(H_1)Pr(\mathbf{X}|H_1)}{Pr(\mathbf{X})} \tag{3.1}$$

$$Pr(H_0|\mathbf{X}) = \frac{Pr(H_0)Pr(\mathbf{X}|H_0)}{Pr(\mathbf{X})} \tag{3.2}$$

Assume there are N spheres and denote the location of the i-th sphere by $\mathbf{X}_i$. As we stated previously, the probability function is correspond to Gaussian laws of mean (x_i, y_i, z_i) and variance σ^2. Here we assume the noise is white.

$$Pr(\mathbf{X_i}|H_0) = \frac{1}{(2\pi\sigma^2)^{\frac{3}{2}}}\mathbf{exp}(-\frac{(x-x_i)^2+(y-y_i)^2+(z-z_i)^2}{2\sigma^2}) \tag{3.3}$$

By computing the Norm of the location of the $i-th$ sphere in the time series, we can obtain the likelihood function for the $i-th$ sphere. $\mathbf{X}_i(t)$ is the observed blobs location vector in consecutive frames. u_i is the mean value for these observed blobs location vector.

$$Pr(\mathbf{X}_i(t)) = \begin{cases} \frac{1}{(2\pi\sigma^2)^{\frac{3}{2}}}\mathbf{exp}(-\frac{||(\mathbf{X}_i(t)-u_i)||^2}{2\sigma^2}) & \text{if } 0 \le t \le t'-1, \\ \frac{1}{(2\pi\sigma^2)^{\frac{3}{2}}}\mathbf{exp}(-\frac{||(\mathbf{X}_i(t)-u_i-\Delta)||^2}{2\sigma^2}) & \text{if } t' \le t \le T-1. \end{cases} \tag{3.4}$$

The joint probability distribution of N spheres in time series can be expressed as following:

$$Pr(\mathbf{X}_0(t), \mathbf{X}_1(t), ..., \mathbf{X}_{N-1}(t)) = \prod_{i=0}^{N-1} Pr(\mathbf{X}_i(t)) \tag{3.5}$$

Let us denote the likelihood function L_0 associated with hypothesis H_0, and the likelihood function L_1 associated with hypothesis H_1. After each hypothesis is expressed in statistical terms, L_0 and L_1 can be inferred from the maximum probability of

$$L_0 = MAX_{\{u_i\}}\{Pr(\mathbf{X}_0(0, 1, ..., T-1), \mathbf{X}_1(0, 1, ..., T-1), ..., \mathbf{X}_{N-1}(0, 1, ..., T-1))\} \tag{3.6}$$

$$L_1 = MAX_{\{u_i, t', \Delta\}}\{Pr(\mathbf{X}_0(0, 1, ..., t'-1), ..., \mathbf{X}_{N-1}(0, 1, ..., t'-1), \mathbf{X}_0(t', ..., T-1), ..., \mathbf{X}_{N-1}(t', ..., T-1))\} \tag{3.7}$$

That is to say, for hypothesis H_0 and H_1, the maximum joint probability also can be expressed as follows,

$$L_0 = MAX_{\{u_i\}} \prod_{t=0}^{T-1} \prod_{i=0}^{N-1} Pr(\mathbf{X}_i(t)) \tag{3.8}$$

$$L_1 = MAX_{\{u_i, t', \Delta\}}\{\prod_{t=0}^{t'-1} \prod_{i=0}^{N-1} Pr(\mathbf{X}_i(t))\}\{\prod_{t=t'}^{T-1} \prod_{i=0}^{N-1} Pr(\mathbf{X}_i(t))\} \tag{3.9}$$

In the equation (3.9) we assume there certainly has one motion in time t'. With comparing the result L_1 and L_0 and computing them recursively, we will make the final motion decision for the SPECT frames.

3.3 The Signal-To-Noise Ratio

The Signal-to-Noise Ratio is one important factor to measure the splitting frames strategy. Signal-to-Noise Ratio(SNR) is the mean power carried by the meaningful information divided by the mean power carried by the noise:

$$SNR(dB) = 10log_{10}(P_{signal}/P_{noise}) \tag{3.10}$$

We compute SNR for different case studies to measure the performance.

CHAPTER 4

SPLITTING FRAMES FOR MOTION COMPENSATION

4.1 Algorithm Description

In Chapter 3, the basic splitting frames algorithm is designed. The algorithm description is as following:

Algorithm SFA I (spheres_locations, timestamps, frames numbers N)

1. With the no-motion hypothesis, calculate the maximum joint Gaussian distribution probability L_0 of m spheres for n sub-frames in time series.

2. With the one-motion hypothesis in the i-th sub-frame, calculate the maximum joint probability L_1 of m spheres for the first $(i-1)$ sub-frames and the other $(n-i+1)$ sub-frames.

3. If the frame splitting criterion is met ($L_1 > L_0$), do the splitting operation at the i-th sub-frame, otherwise process new input data or exit the SFA algorithm.

4. After the splitting operation, treat the first $(i-1)$ sub-frames and the other $(n-i+1)$ sub-frames as new frames respectively and perform the SFA algorithm recursively.

This algorithm computation complexity is $O(N^2 lgN)$.

4.2 Speeding Up the Splitting Frames Algorithm

If a large set of input frames(with many spheres in one frame) is utilized, the splitting frames implementation in Chapter 3 is time consuming. Also to take the statistics computation result more reasonable and tractable, we design the fast implementation for it. and will take further log computation for the analysis. From the equation (1), we have:

$$ln(Pr(H_0|\mathbf{X})) = ln(\frac{Pr(H_0)Pr(\mathbf{X}|H_0)}{Pr(\mathbf{X})}) \tag{4.1}$$

$$ln(Pr(H_1|\mathbf{X})) = ln(\frac{Pr(H_1)Pr(\mathbf{X}|H_1)}{Pr(\mathbf{X})}) \tag{4.2}$$

To compare the value of equation (3.8) and equation (3.9), we need to compute $ln((Pr(H_1)Pr(\mathbf{X}|H_1)$ and $ln(Pr(H_0)Pr(\mathbf{X}|H_0))$

From equation (3.3) we have

$$Pr(\mathbf{X}|H_0) = \frac{1}{(2\pi\sigma_0^2)^{\frac{3}{2}}}\mathbf{exp}(-\frac{||\mathbf{X}-\mathbf{X_0})||^2}{2\sigma_0^2}) \tag{4.3}$$

$$Pr(\mathbf{X}|H_1) = \frac{1}{(2\pi\sigma_1^2)^{\frac{3}{2}}}\mathbf{exp}(-\frac{||\mathbf{X}-\mathbf{X_1}||^2}{2\sigma_1^2}) \tag{4.4}$$

If there is no motion, we have

$$ln(Pr(H_0|\mathbf{X})) > ln(Pr(H_1|\mathbf{X})) \tag{4.5}$$

Then

$$ln(Pr(H_0)) - ln(2\pi\sigma_0^2)^{\frac{3}{2}} - \frac{||\mathbf{X}-\mathbf{X_0})||^2}{2\sigma_0^2} > ln(Pr(H_1)) - ln(2\pi\sigma_1^2)^{\frac{3}{2}} - \frac{||(\mathbf{X}-\mathbf{X_1})||^2}{2\sigma_1^2} \tag{4.6}$$

$$ln(\frac{Pr(H_0)}{Pr(H_1)}) + ln(\frac{\sigma_1^3}{\sigma_0^3}) > \frac{1}{2}(\frac{||(\mathbf{X}-\mathbf{X_0})||^2}{\sigma_0^2} - \frac{||(\mathbf{X}-\mathbf{X_1})||^2}{\sigma_1^2}) \tag{4.7}$$

Motion decision threshold $T = ln(\frac{Pr(H_0)}{Pr(H_1)}) + ln(\frac{\sigma_1^3}{\sigma_0^3})$ We assume $\sigma_0 = \sigma_1$, thus motion decision threshold $T = \sigma^2 ln(\frac{Pr(H_0)}{Pr(H_1)})$. In the multi dimension space, when blobs location X is located above the threshold space, we will make the motion decision. The Splitting Frames Algorithm(SFA) uses hypothesis testing to decide and reset the frames for the location of blobs on patient body in SPECT. We have two competing hypotheses for patient motion decision and define the likelihood ratio criterion to decide on patient motion.

To speed up the Splitting Frames Algorithm, likelihood computation is also iteratively expressed and converted to linear computation. The computation complexity is $O(n)$ after the conversion.

With the expression of Maximum Likelihood Estimation as follows:

$$L_1 = MAX_{\{u_i,t',\Delta\}}\{\prod_{t=0}^{t'-1}\prod_{i=0}^{N-1} Pr(\mathbf{X}_i(t))\}\{\prod_{t=t'}^{T-1}\prod_{i=0}^{N-1} Pr(\mathbf{X}_i(t))\} \tag{4.8}$$

The non-linear computation can be converted to linear computation as follows:

$$L_1 = MAX_{\{u_i,R,\Delta\}}\{\sum_{t=L}^{R-1}(\mathbf{X}(t) - \bar{\mathbf{X}}_L)^2 \ + \sum_{t=R}^{H}(\mathbf{X}(t) - \bar{\mathbf{X}}_H)^2\} \tag{4.9}$$

Where L, R and H are variance based on the recursive computation.

$$\begin{aligned}\sum_{t=L}^{R-1}(\mathbf{X}(t) - \bar{\mathbf{X}}_L)^2 \ &= \sum_{t=L}^{R-1}((\mathbf{X}(t))^2 + (\bar{\mathbf{X}}_L)^2 - 2\mathbf{X}(t)\bar{\mathbf{X}}_L) \\ &= \sum_{t=L}^{R-1}(\mathbf{X}(t))^2 + (R-L)\bar{\mathbf{X}}_L^2 - 2\bar{\mathbf{X}}_L(R-L)\bar{\mathbf{X}}_L \\ &= \sum_{t=L}^{R-1}(\mathbf{X}(t))^2 - (R-L)\bar{\mathbf{X}}_L^2\end{aligned} \tag{4.10}$$

Based on this derivation ,we can express L_1 iteratively.

$$\begin{aligned}L_1 &= \sum_{t=L}^{R-1}(\mathbf{X}(t))^2 - (R-L)\bar{\mathbf{X}}_L^2 + \sum_{t=R}^{H}(\mathbf{X}(t))^2 - (H-R+1)\bar{\mathbf{X}}_H^2 \\ &= \sum_{t=L}^{H}(\mathbf{X}(t))^2 - ((R-L)\bar{\mathbf{X}}_L^2 + (H-R+1)\bar{\mathbf{X}}_H^2)\end{aligned} \tag{4.11}$$

With the expression of Maximum Likelihood Estimation as follows:

$$L_1 = MAX_{\{u_i,t',\Delta\}}\{\prod_{t=0}^{t'-1}\prod_{i=0}^{N-1} Pr(\mathbf{X}_i(t))\}\{\prod_{t=t'}^{T-1}\prod_{i=0}^{N-1} Pr(\mathbf{X}_i(t))\} \tag{4.12}$$

The non-linear computation can be converted to linear computation as follows:

$$L_1 = MAX_{\{u_i,R,\Delta\}}\{\sum_{t=L}^{R-1}(\mathbf{X}(t) - \bar{\mathbf{X}}_L)^2 \ + \sum_{t=R}^{H}(\mathbf{X}(t) - \bar{\mathbf{X}}_H)^2\} \tag{4.13}$$

Where L, R and H are variance based on the recursive computation.

$$\begin{aligned}\sum_{t=L}^{R-1}(\mathbf{X}(t) - \bar{\mathbf{X}}_L)^2 \ &= \sum_{t=L}^{R-1}((\mathbf{X}(t))^2 + (\bar{\mathbf{X}}_L)^2 - 2\mathbf{X}(t)\bar{\mathbf{X}}_L) \\ &= \sum_{t=L}^{R-1}(\mathbf{X}(t))^2 + (R-L)\bar{\mathbf{X}}_L^2 - 2\bar{\mathbf{X}}_L(R-L)\bar{\mathbf{X}}_L \\ &= \sum_{t=L}^{R-1}(\mathbf{X}(t))^2 - (R-L)\bar{\mathbf{X}}_L^2\end{aligned} \tag{4.14}$$

Based on this derivation ,we can express L_1 iteratively.

$$\begin{aligned}L_1 &= \sum_{t=L}^{R-1}(\mathbf{X}(t))^2 - (R-L)\bar{\mathbf{X}}_L^2 + \sum_{t=R}^{H}(\mathbf{X}(t))^2 - (H-R+1)\bar{\mathbf{X}}_H^2 \\ &= \sum_{t=L}^{H}(\mathbf{X}(t))^2 - ((R-L)\bar{\mathbf{X}}_L^2 + (H-R+1)\bar{\mathbf{X}}_H^2)\end{aligned} \tag{4.15}$$

The pseudo code is as follows:

---

sum1 = 0;

sum2 = $\sum_{t=L}^{H}(\mathbf{X}(t))^2$;

for(R = L; R <= H; R++)

{

sum1 = sum1 + X(R);

sum2 = sum1 - X(R);

$\bar{X}_L$ = sum1 / (R - L);

$\bar{X}_H$ = sum2 / (H - R + 1);

L(R) = $\sum_{t=L}^{H}(\mathbf{X}(t))^2 - ((R-L)\bar{\mathbf{X}}_L^2 + (H-R+1)\bar{\mathbf{X}}_H^2)$

}

In this fast implementation, the motion decision can be made in linear complexity O(N).

CHAPTER 5

EXPERIMENTS AND CASE STUDIES

In chapter 3 and chapter 4, the splitting frames algorithm is represented. Some simulation experiments, case studies and analysis will be showed in this chapter.

5.1 Case Study I

Simulation results are shown in Figures 5.1 and 5.2. Figure 5.1 shows the time-varying positions of markers in the presence of patient motion. The hierarchical steps to split frames for motion compensation are presented in Figure 5.2, where the probability L_1 for every possible motion time instant is shown.

There are 150 simulated data points in Figure 5.2. In (a), the probability L_1 for every possible motion during the first scan is shown, which is denoted by "Level 1" in the figure. From the figure, we can see that the L_1 at time 120 is the largest. So there is one motion at $t' = 120$. We then divide the input data into two frames [1, 119] and [120, 150], and apply the same frame splitting algorithm.

There is no motion detected for the second part. The L_1 results for the first part [1, 119] are shown in (b) as "Level 2". We can easily see from (b) that there is one motion at $t' = 90$. The first part [1,119] is then divided into [1, 89] and [90, 119], and our splitting frame algorithm is applied to them respectively until all motions are found.

There are four motions in the input simulated patient position data, and the detections by our splitting frame algorithm are shown in Figure 5.2 from "Level 1" to "Level 4".

5.2 Case Study II

Another experimental results are shown in Figure 5.3, Figure 5.4, Figure 5.6 and Figure 5.5. Figure 5.3 shows the time-varying positions of markers in the presence of patient

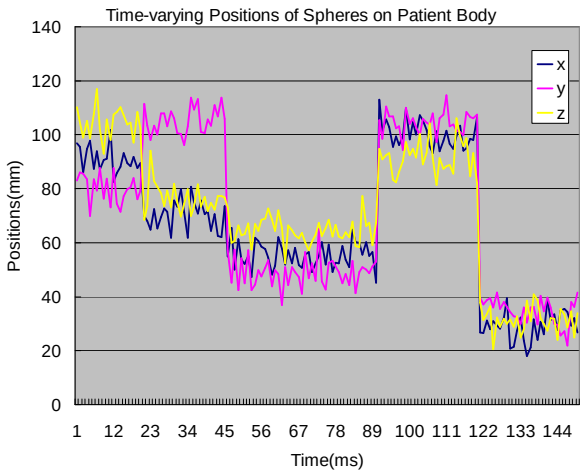

Figure 5.1. Time-varying Positions of Spheres on Patient Body in SPECT

motion. In Figure 5.4, the three dimension components of time-varying positions of markers are shown. The hierarchical steps to split frames for motion compensation are presented in Figure 5.5, where the probability L_1 for every possible motion time instants is shown.

There are 150 simulated data points in Figure 5.5. In (a), the probability L_1 for every possible motion during the first scan is shown, which is denoted by "Level 1" in the figure. From the figure, we can see that the L_1 at time 120 is the largest. So there is one motion at $t' = 120$. We then divide the input data into two frames [1, 119] and [120, 150], and apply the same frame splitting algorithm.

There is no motion detected for the second part. The L_1 results for the first part [1, 119] are shown in (b) as "Level 2". We can easily see from (b) that there is one motion at $t' = 90$. The first part [1,119] is then divided into [1, 89] and [90, 119], and our splitting frame algorithm is applied to them respectively until all motions are found.

There are four motions in the input simulated patient position data, and the detections by our splitting frame algorithm are shown in Figure 5.5 from "Level 1" to "Level 4". The corrected patient positions after splitting frames and resetting motions are shown in Figure 5.6, which are averaged during the intervals between consecutive motions.

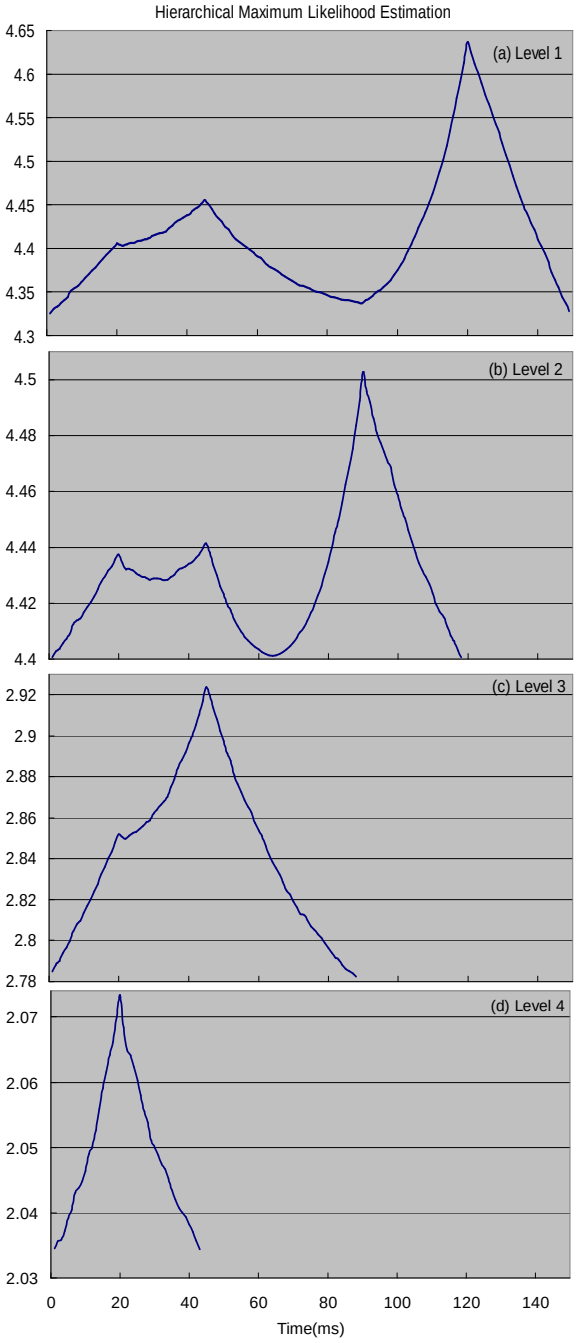

Figure 5.2. Hierarchical Maximum Likelihood Estimation for Splitting Frames

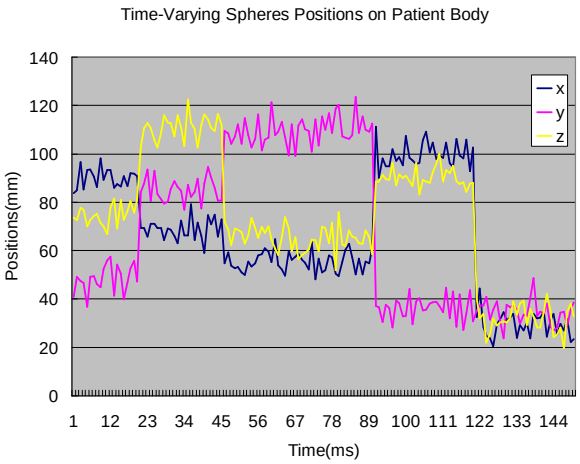

Figure 5.3. Time-varying Positions of Spheres on Patient Body in SPECT

5.3 Case Study III

Another experimental results are shown in Figure 5.7, Figure 5.9, Figure 5.10, Figure 5.11, Figure 5.12, and Figure 5.8. Figure 5.7 shows the Y component of time-varying positions of markers in the presence of patient motion. The hierarchical steps to split frames for motion compensation are presented in Figure 5.9, Figure 5.10, Figure 5.11, and Figure 5.12, where the probability L_1 for every possible motion time instant is shown.

There are 30000 simulated data points in Figure 5.7. In Figure 5.9, the probability L_1 for every possible motion during the first scan is shown. From the figure, we can see that the L_1 at time 15000 is the largest. So there is one motion at $t' = 15000$. We then divide the input data into two frames [1, 14999] and [15000, 30000], and apply the same frame splitting algorithm.

Continuing this process, we are able to find all patient motions. There is one motion detected for the second part (time interval [15000, 30000]). And there are two motions detected for the first part (time interval [1, 14999]). There are four motions in the input simulated patient position data, and the detections by our splitting frame algorithm are shown in Figure 5.9 to Figure 5.12. The corrected patient positions after splitting frames and resetting motions are shown in Figure 5.8.

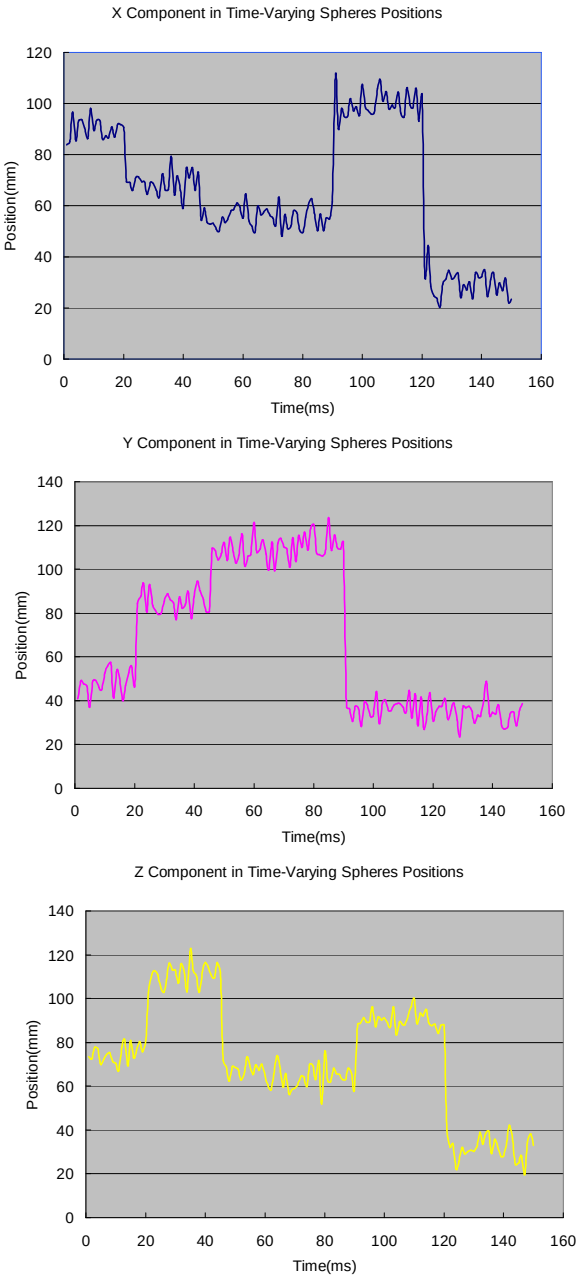

Figure 5.4. Time-varying Positions Components of Spheres

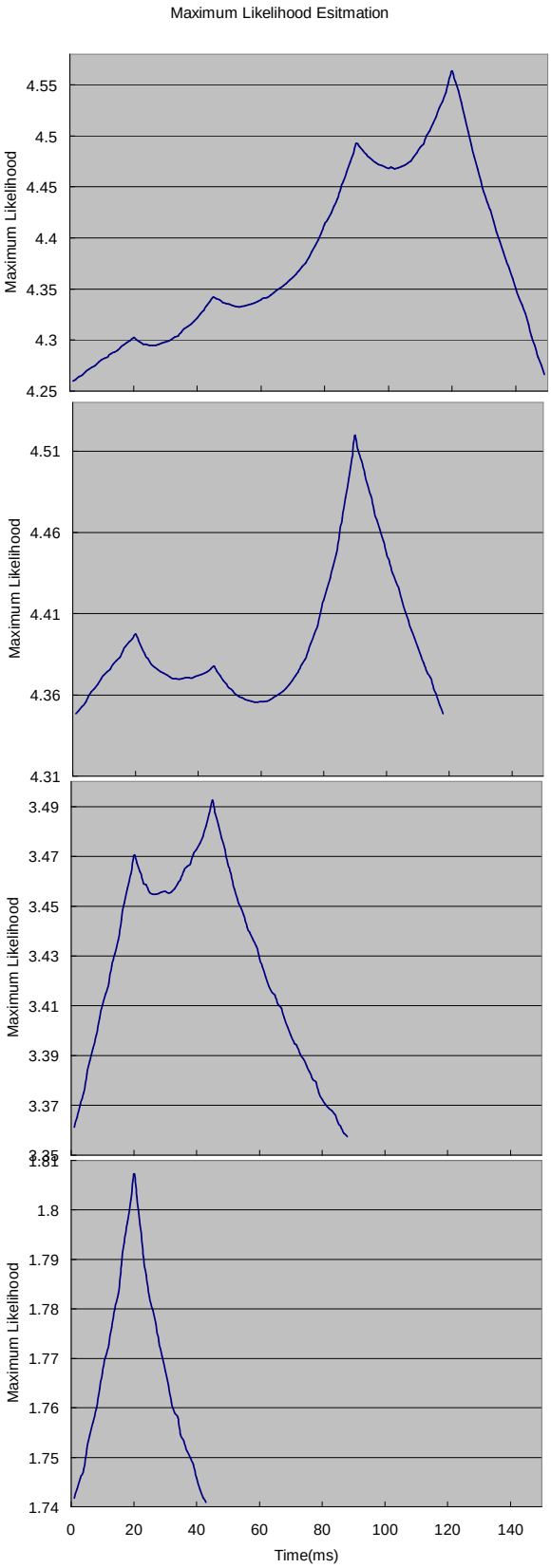

Figure 5.5. Hierarchical Maximum Likelihood Estimation for Splitting Frames

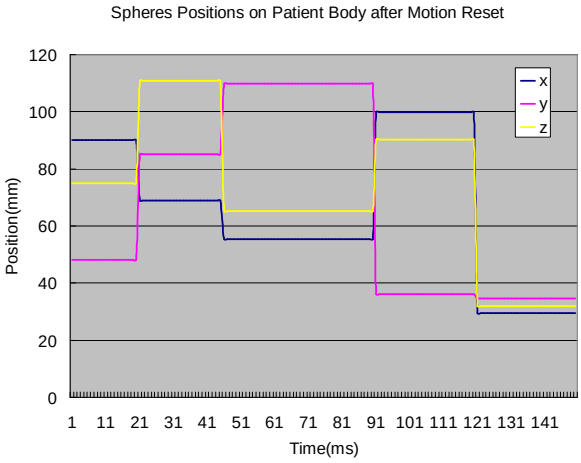

Figure 5.6. Corrected Positions after Splitting Frames and Resetting Motion

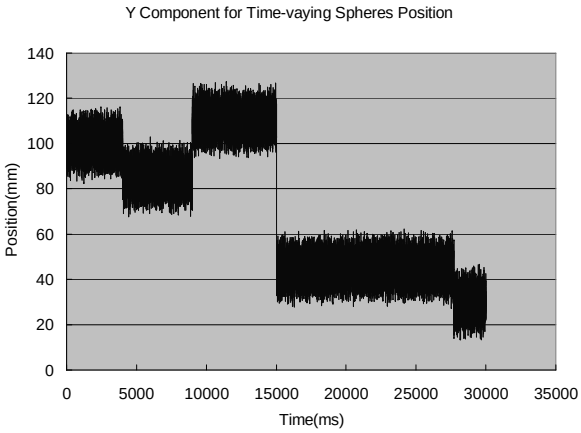

Figure 5.7. Large Scale Motion Case Studies

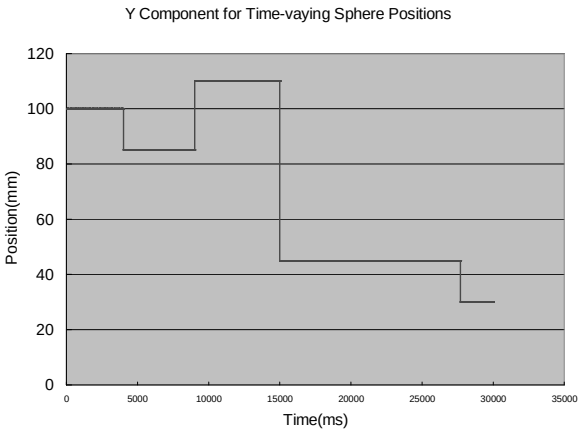

Figure 5.8. Corrected Positions after Splitting Frames and Resetting Motion

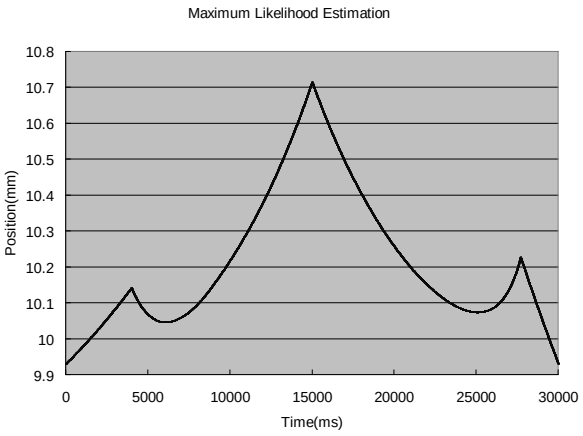

Figure 5.9. Maximum Likelihood Estimation for Time Interval [1, 30000]

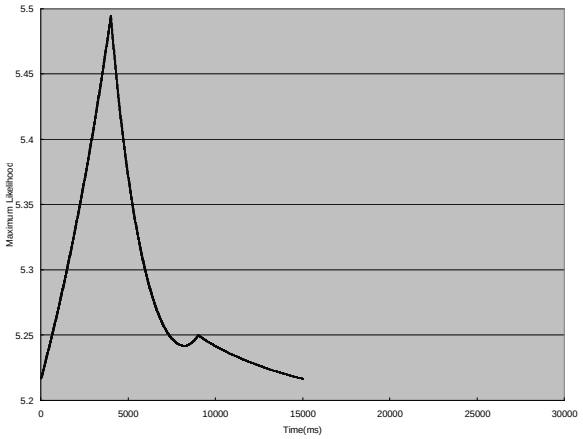

Figure 5.10. Maximum Likelihood Estimation for Time Interval [1, 14999]

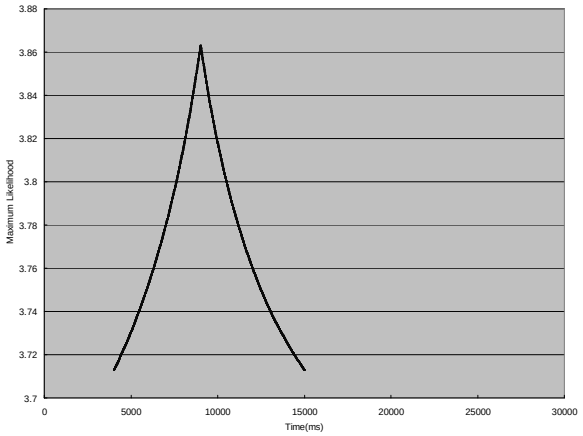

Figure 5.11. Maximum Likelihood Estimation for Time Interval [8000, 14999]

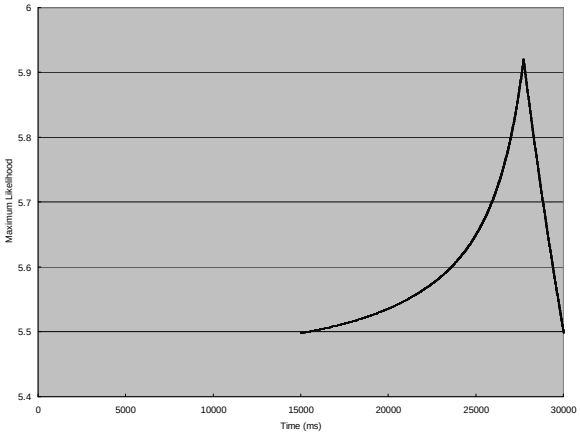

Figure 5.12. Maximum Likelihood Estimation for Time Interval [15000, 30000]

5.4 Case Study IV

Another experimental results are shown in Figure 5.13, Figure 5.14, and Figure 5.15. Figure 5.13 shows the time-varying positions of markers in the presence of patient motion. In Figure 5.14, the X component of time-varying positions of markers is shown. The hierarchical steps to split frames for motion compensation are presented in Figure 5.15, where the probability L_1 for the possible motion time instants is shown.

From Figure 5.13, we can see there is a large jump in patient positions at time 75, and the positions go back at time 76. So this jump is actually caused by environmental noise, and it should be detected as a false motion.

There are 150 simulated data points in Figure 5.15. From the figure, we can see that The L_1 at time 75 and 76 is not the largest. And the L_1 at time 72 is the largest, but the jump at time 72 is very small. So our splitting frame algorithm will not stop here, and output no motion. This is the desired result.

Another experimental results are shown in Figure 5.16, Figure 5.17, and Figure 5.18. Figure 5.16 shows the time-varying positions of markers in the presence of patient motion. The hierarchical steps to split frames for motion compensation are presented in Figure 5.15, where the probability L_1 for the possible motion time instants is shown. The corrected patient positions after splitting frames and resetting motions are shown in Figure 5.18.

From Figure 5.16, we can see there is a large jump in patient positions at time 75, and the positions stay there for 5 time intervals and go back at time 80. So this jump is a real

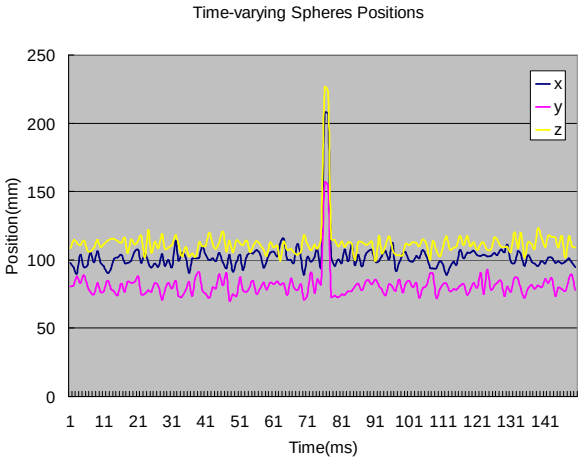

Figure 5.13. Time-varying Positions of Spheres on Patient Body in SPECT

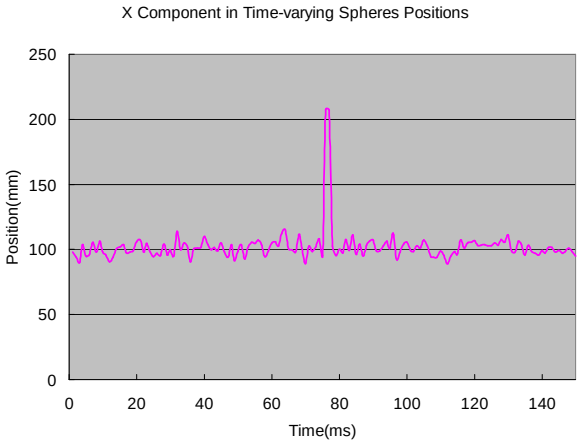

Figure 5.14. The X component of Time-varying Positions of Spheres on Patient Body in SPECT

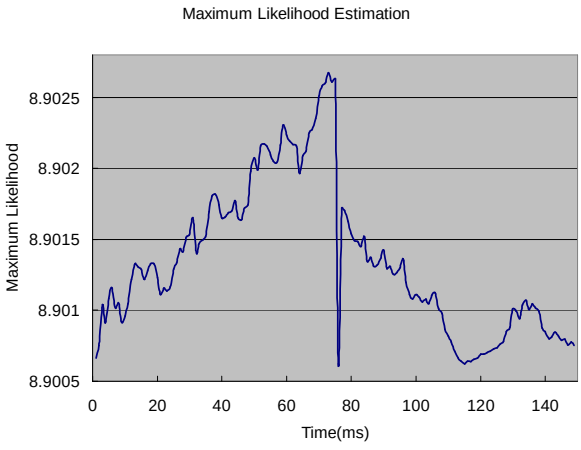

Figure 5.15. Maximum Likelihood Estimation for Splitting Frames

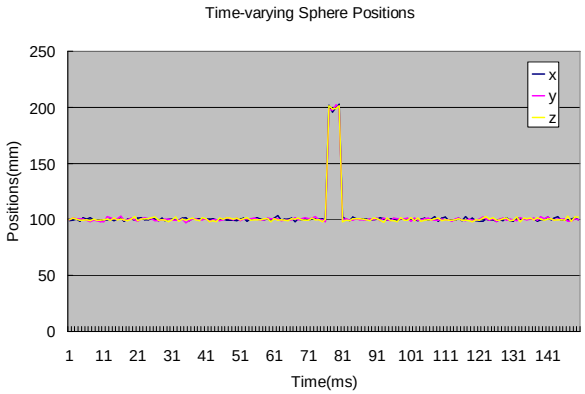

Figure 5.16. Time-varying Positions of Spheres on Patient Body in SPECT

patient move, which is not caused by environmental noise, and it should be detected as a real motion.

There are 150 simulated data points totally in Figure 5.5. In (a), the probability L_1 for every possible motion during the first scan is shown, which is denoted by "Level 1" in the figure. From the figure, we can see that the L_1 at time 75 is the largest. So there is one motion at time=75. We then divide the input data into two frames [1, 74] and [75, 150], and apply the same frame splitting algorithm.

There is no motion detected for the first part, and we do not show the results for the first part for brevity. The L_1 results for the seconde part [75, 150] are shown in (b), which is denoted by "Level 2". We can easily see from (b) that there is one motion at time=80. The second part [75, 150] is then divided into [75, 79] and [80, 150], and our splitting frame algorithm is applied to them again. Because there are no motions in both parts, our splitting frame algorithm will stop, and report all motions found.

There are two motions in the input simulated patient position data, which are found using our splitting frame algorithm as shown in Figure 5.17. The corrected patient positions after splitting frames and resetting motions are shown in Figure 5.18.

5.5 Discussion

In the splitting frames problems for motion compensation in SPECT, the hypotheses are verified to make decision. We have studied the basic statistical algorithm and optimized

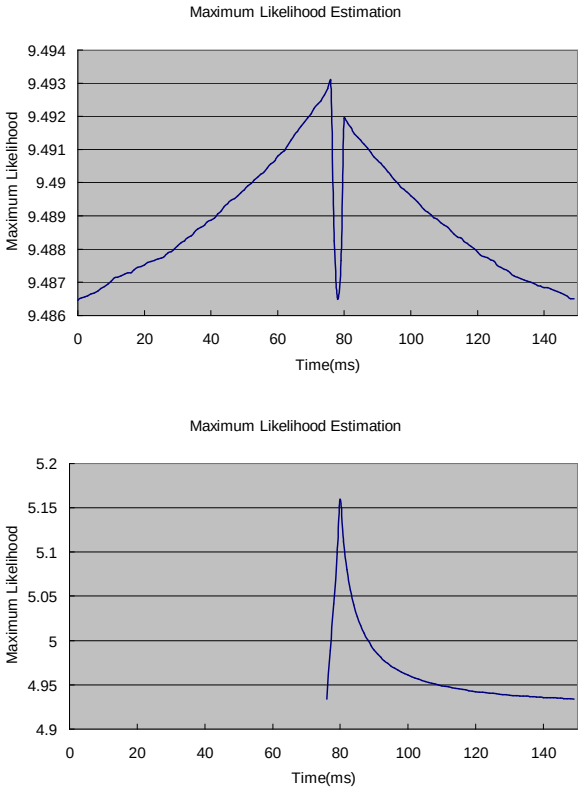

Figure 5.17. Hierarchical Maximum Likelihood Estimation for Splitting Frames

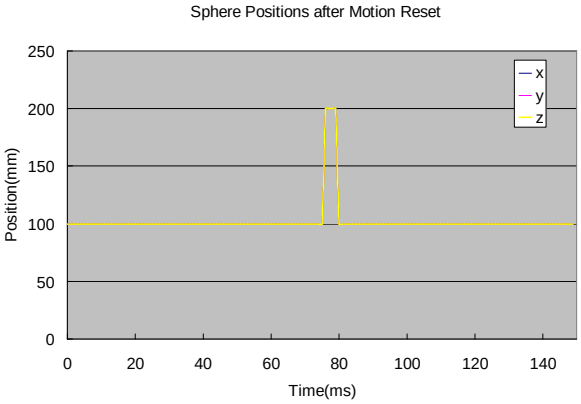

Figure 5.18. Corrected Patient Positions after Splitting Frames and Resetting Motion

algorithm for this problem. The recursive computation verifies the hypotheses at each iteration, regarding the state sequence as unobserved data. The algorithm can filter the impulse noise in sequences. This property of the algorithm is useful, because patient motion is not recognized until the position value is held for a while. Also the performance of the algorithm should be climbing with shorter time in SPECT, usually 15 minutes in the practical application, with the small data sets.

CHAPTER 6

CONCLUSION

6.1 Conclusion

The hypothesis testing based method has been taken for splitting frames problem for motion compensation in SPECT. [9]The Bayesian recursive estimation methods are applied in our decision. In the splitting frames algorithm after converting to linear computation and iteratively expression likelihood value, the performance is good for sample SNR. Even if the recursive computation is somehow time-consuming, the simulations in large scale data show the acceptable results after optimizing implementation. Different motion cases are discussed as well to verify the algorithm accuracy. Simulation experiment results demonstrate this accurate and efficient splitting frames algorithm. The results from this work show that this type complex problem can be handled with the statistical Bayesian method. One of the future challenges is to apply this algorithm to the practical SPECT and VTS system.

6.2 Future Work

In our implementation, we assume the problem is based on Gaussian distribution. The conceptual recursive update of the posterior status works very well, but it should be very hard to implement when the problem is of nonlinear and non-Gaussian character. A trade off between making decision accuracy and implementing complexity is controlled under sample SNR in simulating implementations. The algorithm can be used in the verification of 3D sphere motion decision, as well as the verification of 2D blobs motion decision. In future, we can continue to construct some probability density functions to measure the splitting frames reliability. There are a lot interesting problems left to solve, both theoretical and practical area.

BIBLIOGRAPHY

[1] Bretthorst, G. Larry, 1988, Bayesian Spectrum Analysis and Parameter Estimation in Lecture Notes in Statistics, 48, Springer-Verlag, New York, New York;

[2] B.Feng, H.C. Gifford, R.D. Beach, G. Boening, M.A. Gennert, M.A. King, "Use of the three-dimensional Gaussian interpolation in the projector/backprojector pair for compensation of the known rigid-body motion in SPECT," In Fully Three-Dimensional Image Reconstruction Meeting on Radiology and Nuclear Medicine, Salt Lake City, July, 2005.

[3] E.H.Botvinick, Y.Y. Zhu, W.J. O'Connell and M.W. Dae, "A quantitative assessment of patient motion and its effect on myocardial perfusion SPECT images," Journal of Nuclear Medicine, Vol. 34, Issue 2, 303-310, Feb. 1993.

[4] F.M. Prigent, M. Hyun, D.S. Berman and A. Rozanski, "Effect of motion on thallium-201 SPECT studies: a simulation and clinical study," Journal of Nuclear Medicine, Vol. 34, Issue 11 1845-1850, Nov. 1993.

[5] Jaynes, E.T. (1998) Probability Theory : The Logic of Science

[6] J.D. Morgenstern, M.A. Gennert, S. Nadella, N. Kumar, G.C. Speckert, P.P. Bruyant, M.A. King. "A real time multi-threaded system to detect patient motion in SPECT imaging using multiple optical cameras." Medical Imaging Conference IEEE 2004 Rome, Italy - M5-74.

[7] J. Fitzgerald and P. G. Danias, "Effect of motion on cardiac SPECT imaging: recognition and motion correction." J. Nucl. Cardiol, vol.8, no. 6, pp.701-706, Nov.2001

[8] L. Ma, S. Gu, S. Nadella, P.P. Bruyant, M.A. King, M.A. Gennert, A practical rebinning-based method for patient motion in SPECT imaging, Int. Conf. Computer Graphics, Imaging and Visualization, Beijing, China, July 2005.

[9] L. Ma, B. Feng, J. McNamara, M.A. Gennert, M.A. King, Splitting Frames Based on Hypothesis Testing for Patient Motion Compensation in SPECT, Accepted in IEEE Nuclear Science Symposium and Medical Imaging Conference, California, Nov, 2006.

[10] ME Casey, H Gadagkar and D Newport 1995 "A component based method for normalisation in volume PET" Proceedings of the 3rd International Meeting on Fully Three-Dimensional Image Reconstruction in Radiology and Nuclear Medicine, Aix-les-Bains, France.

[11] Matsumoto N, Berman DS, Kavanagh PB, Gerlach J, Hayes SW, Lewin HC, Friedman JD, Germano G. "Quantitative assessment of motion artifacts and validation of a new motion-correction program for myocardial perfusion SPECT." J Nucl Med. 2001 May;42(5):687-94.

[12] M.A. Gennert, P.P. Bruyant, M.V. Narayanan, and M.A. King. "Assessing a system to detect patient motion in SPECT imaging using stereo optical cameras." Nuclear Science Symposium Conference Record, 2002 IEEE , Volume: 3 , 10-16 Nov 2002 Page(s): 1567 -1570. IEEE

[13] MH Hudson, RS Larkin, "Accelerated image reconstruction using ordered subsets of projection data." IEEE Trans Med Imaging vol 13, pp. 601-609, 1994.

[14] P.P. Bruyant, M.A. Gennert, G.C. Speckert, R.D. Beach, J.D. Morgenstern, N. Kumar, S. Nadella and M.A. King. "A robust visual tracking system for motion detection in SPECT: Hardware solutions." Medical Imaging Conference IEEE 2004 Rome, Italy - M5-266.

[15] P.P. Bruyant, M.A. Gennert, G.C. Speckert, R.D. Beach, J.D. Morgenstern, N. Kumar, S. Nadella, M.A. King, "A Robust Visual Tracking System for Motion Detection in SPECT: Hardware Solutions," In IEEE Trans. Nuclear Science, 2005.

[16] Pellot-Barakat, M. Ivanovich, D. A. Weber, A. Herment, D. K. Shelton; "Motion Detection of Motion in Triple Scan SPECT Imaging"; 0018-9499, 1998, IEEE Trans. Nucl. Sci., vol. 45(4): pp. 2238-2244, August 1998.

[17] R. Eisner, A. Churchwell, T. Noever, D. Nowak, K. Cloninger, D. Dunn, W. Carlson, J. Oates, J. Jones and D. Morris, "Quantitative analysis of the tomographic thallium-201 myocardial bullseye display: critical role of correcting for patient motion," Journal of Nuclear Medicine, Vol. 29, Issue 1 91-97, Jan. 1988

[18] R R Fulton, B F Hutton, M Braun, B Ardekani and R Larkin, "Use of 3D reconstruction to correct for patient motion in SPECT", Phys. Med. Biol. 39 563-574 1994.

[19] R.R.Fulton, S.Eberl, S.R.Meikle, B.F.Hutton, and M. Braun, "A practical 3D tomographic method for correcting patient head motion in clinical SPECT." IEEE Trans. Nucl. Sci., vol. 46: pp. 667-672, June 1999.

[20] William J. Geckle, Terry L. Frank, Jonathan M. links and Lewis C. becker, "Correction for Patient and Organ Movement in SPECT: Application to Exercise Thallium-201 Cardiac Imaging", J. Nucl. Med. Vol. 29, PP:441- 450, 1995

[21] Zellner, A., (1980), in Bayesian Statistics, J. M. Bernardo, ed., Valencia Univer- sity Press, Valencia, Spain.